

Modulated Piezoreflectance in Semiconductors*

ANIBAL GAVINI† AND MANUEL CARDONA

Department of Physics, Brown University, Providence, Rhode Island 02912

(Received 24 July 1969)

The direct gaps of Ge, GaAs, GaSb, InP, ZnS, CdTe, CdSe, CdS, and ZnO have been measured using the piezoreflectance technique. Thin single crystals of these materials were mounted on lead-zirconate-lead-titanate piezoelectric transducers and cooled to 77°K. Measurements were performed with the stress applied along the [100] and [111] crystallographic directions of the cubic materials and along the [0001] and [1120] directions of the hexagonal materials. The shear deformation potentials b and d of the highest valence-band state of the cubic materials were determined from the ratio of the intensity of the light polarized parallel and perpendicular to the direction of the stress and the known values of the hydrostatic deformation potentials. The results show a continuous increase of the ratio d/b from the covalent materials Ge and Si to the partially ionic III-V and II-VI compounds. A simple point-ion model is proposed to explain the increase in the ratio d/b with increasing ionicity for the cubic materials. For the wurtzite materials, similar measurements yield ratios of shear to hydrostatic deformation potentials. Information about the stress-exchange splittings and the corresponding exchange-interaction constant is also obtained.

I. INTRODUCTION

THE study of optical critical-point structure in solids by means of modulation (i.e., differential) techniques has received considerable attention. The techniques of electroreflectance,^{1,2} electroabsorption,³ thermoreflectance,^{4,5} piezoreflectance,⁶⁻⁸ and piezoabsorption⁹ have been applied to semiconductors, metals, and insulators. Absorption modulation methods^{3,9} are most useful for studying indirect transitions below the lowest direct gap, while reflection modulation is normally used for studying allowed direct transitions.

Some of the modulation techniques mentioned (temperature modulation, hydrostatic-pressure modulation) preserve the symmetry of the crystal. When applied to cubic materials, they yield spectra independent of the direction of polarization of the light. Other techniques (uniaxial-stress modulation, electric field modulation) lower the crystal symmetry and give anisotropic spectra. In this case, information about the symmetry of the transitions involved can be obtained.

We have chosen for the work reported here the uniaxial-stress technique of piezoreflectance. The signals obtained by this method are typically an order of magnitude smaller than those obtained with electroreflectance,

and very often a relatively large background due to mechanical vibrations of the system is present. The interpretation of the results of piezoreflectance, however, is rather straightforward when compared to electroreflectance, since the stress preserves the translational invariance of the crystal (while the electric field does not): The line shape of the piezoreflectance structure is essentially the derivative of the corresponding structure in the static optical properties. By comparing the strength of the signals observed for various directions of polarization, information about deformation potentials can be obtained.

Several methods have been used for applying a modulated stress. Engeler *et al.*⁶ measured Si, Ge, and GaAs, and Garfinkel *et al.*¹⁰ measured the noble metals by stressing single crystals or evaporated films with a piezoelectric transducer. Gerhardt *et al.*^{7,11} measured KI, KBr, and Cu with the crystals stressed by periodic bending at low frequencies. Two systems which permit the simultaneous application of a large static stress and a small modulation have been reported. In Balslev's system,¹² the static stress is applied with weights and the modulating stress with an arrangement similar to the coil and magnet of a dynamic loudspeaker. Sell and Kane¹³ used a pneumatic piston system for applying both modulation and static stress.

We have used the technique of Engeler *et al.*⁶ slightly modified so as to produce a uniform strain. Thin samples of Ge, GaAs, GaSb, InP, CdTe, ZnS, CdSe, CdS, and ZnO were mounted on a lead-titanate-lead-zirconate piezoelectric transducer (PZT) with only the ends fastened to the transducer so as to obtain a uniform stress of a predetermined direction at the center of the sample. We have studied the piezoreflectance spectra of the direct edge at $\mathbf{k}=0$ (E_0 edge) of those materials for

* Work supported by the National Science Foundation and the Army Research Office, Durham, N. C.

† Present address: Physics Department, McMaster University, Hamilton, Ontario, Canada.

¹ B. O. Seraphin and R. B. Hess, *Phys. Rev. Letters* **14**, 138 (1965).

² M. Cardona, K. L. Shaklee, and F. H. Pollak, *Phys. Rev.* **154**, 696 (1967).

³ A. Frova, P. Handler, F. Germano, and D. E. Aspnes, *Phys. Rev.* **145**, 575 (1966).

⁴ B. Batz, *Solid State Commun.* **4**, 241 (1966); **5**, 985 (1967).

⁵ E. Matatagui, A. Thompson, and M. Cardona, *Phys. Rev.* **176**, 950 (1968).

⁶ W. Engeler, H. Fritzsche, M. Garfinkel, and J. J. Tiemann, *Phys. Rev. Letters* **14**, 1069 (1965).

⁷ U. Gerhardt, D. Beagehole, and R. Sandrock, *Phys. Rev. Letters* **19**, 309 (1967).

⁸ I. Balslev, *Solid State Commun.* **5**, 315 (1967).

⁹ I. Balslev, *Phys. Letters* **24A**, 113 (1967).

¹⁰ M. Garfinkel, J. J. Tiemann, and W. Engeler, *Phys. Rev.* **148**, 695 (1966).

¹¹ U. Gerhardt and M. Mohler, *Phys. Status Solidi* **18**, K45 (1966).

¹² I. Balslev, *Rev. Sci. Instr.* **38**, 1528 (1967).

¹³ D. D. Sell and E. O. Kane, *Phys. Rev.* **185**, 1103 (1969).

light polarized with the electric field (\mathbf{E}) parallel and perpendicular to the stress direction. Measurements were performed with the stress along $[111]$ and along $[100]$ for the cubic materials (Ge, GaAs, GaSb, CdTe, InP, and ZnS). For the hexagonal materials (CdSe, CdS, and ZnO) the stress directions used were the $[0001]$ and the $[11\bar{2}0]$. The $[11\bar{2}0]$ stress measurements were performed with reflecting surfaces either parallel or perpendicular to the c axis.

From the measurements for cubic materials the ratios b/a and d/a of the shear deformation potentials b and d of the top valence state ($\Gamma_{25'}$ or Γ_{15}) to the hydrostatic deformation potential a of the E_0 gap have been found.¹⁴ The hydrostatic deformation potentials are usually known from independent measurements and, hence, b and d can be obtained. The ratio d/b can be found without prior knowledge of a . This ratio shows a monotonic increase from the covalent group-IV elements to the partially ionic III-V and II-VI compounds. It has been suggested earlier¹⁵ that the change in the Coulomb (or Madelung) potential of the displaced ions of the strained material, acting on the anisotropic p -like wave function of the Γ_{15} (or $\Gamma_{25'}$) valence band, should contribute to b and d in partially ionic materials. This contribution dominates the deformation potentials b and d of strongly ionic materials, such as the alkali halides.¹⁵ A simple calculation, based on a point-ion model, explains the increase in d/b with ionicity observed for the germanium-zinc-blende family.

For the wurtzite-type materials, a comparison of the strength of the various piezoreflectance peaks observed for the stress applied along the c axis and perpendicular to it yields two relationships between four deformation potentials.¹⁶ The measurements with a reflecting face perpendicular to the c axis yield information about the stress-exchange splitting and the exchange-interaction constant.^{17,18}

II. THEORY

A. Piezoreflectance

The change $\Delta\epsilon$ in the dielectric-constant tensor produced by the application of a small stress can be written as

$$\Delta\epsilon = \Delta\epsilon_r + i\Delta\epsilon_i = \mathbf{W} \cdot \mathbf{e}, \quad (1)$$

where $\Delta\epsilon_r$ and $\Delta\epsilon_i$ are the real and the imaginary components of $\Delta\epsilon$, \mathbf{e} is the strain tensor, and \mathbf{W} is the fourth-rank strain optical tensor. The components of \mathbf{W} , W_{ijkl} ,

¹⁴ G. Pikus and G. Bir, Fiz. Tverd. Tela **1**, 154 (1959); **1**, 1642 (1959) [English transl.: Soviet Phys.—Solid State **1**, 136 (1959); **1**, 1502 (1960)].

¹⁵ A. Gavini and M. Cardona, Phys. Rev. **177**, 1351 (1969).

¹⁶ G. Pikus, Zh. Eksperim. i Teor. Fiz. **41**, 1507 (1961) [English transl.: Soviet Phys.—JETP **14**, 1075 (1962)]; V. B. Sandomirskii, Fiz. Tverd. Tela **6**, 324 (1963) [English transl.: Soviet Phys.—Solid State **6**, 261 (1964)].

¹⁷ T. Koda and D. W. Langer, Phys. Rev. Letters **20**, 50 (1968).

¹⁸ O. Akimoto and H. Hasegawa, Phys. Rev. Letters **20**, 916 (1968).

are complex numbers. For germanium and zinc blende, \mathbf{W} has three independent components; for wurtzite, it has six. The components of \mathbf{e} are related to those of the stress tensor \mathbf{X} through the elastic-compliance tensor \mathbf{S} : $e_{kl} = S_{klmn}X_{mn}$ with the conventional summation over repeated indices. In a cubic material, the piezoreflectance signal for an arbitrary direction of the electric field of the light \mathbf{n} can be obtained from the piezoreflectance tensor $\Delta\mathbf{R}$:

$$(\Delta R/R)_n = \mathbf{n} \cdot \Delta\mathbf{R} \cdot \mathbf{n}, \quad (2)$$

with

$$\Delta\mathbf{R} = \beta_r \Delta\epsilon_r + \beta_i \Delta\epsilon_i.$$

The real and scalar functions β_r and β_i are the scalar functions α and β of Seraphin and Bottka.¹⁹ We shall calculate $\Delta\epsilon$ for transitions in the vicinity of the E_0 edge. We assume for this doubly degenerate M_0 edge the shape

$$\epsilon \propto i(\omega - \omega_0)^{1/2} + \text{const.} \quad (3)$$

There are two singular contributions to $\Delta\epsilon$. One is produced by the change of oscillator strength [i.e., the omitted proportionality constant of Eq. (3)], and the other is related to the change in ω_0 . The contribution of the change in oscillator strength has the same shape as Eq. (3). We shall neglect it in our analysis in comparison with the signal proportional to $(\omega - \omega_0)^{-1/2}$ produced by $\Delta\omega_0$. The change with stress of the E_0 gap and its spin-orbit split mate $E_0 + \Delta_0$ is governed by the Hamiltonian^{14,20}

$$H = a(e_{xx} + e_{yy} + e_{zz}) - 3b[(L_x^2 - \frac{1}{3}L^2)e_{xx} + \text{cyc. perm.}] - 2\sqrt{3}d[\{L_x, L_y\}e_{xy} + \text{cyc. perm.}], \quad (4)$$

where a , b , and d are deformation potentials, and L_i are the components of the angular momentum operator. For a $[100]$ stress, the valence-band wave functions which diagonalize the Hamiltonian of Eq. (4) are, in the usual angular momentum notation,²⁰

$$\begin{aligned} |\frac{3}{2}, \frac{3}{2}\rangle &= 2^{-1/2}(Y + iZ)\uparrow, \\ |\frac{3}{2}, \frac{1}{2}\rangle &= 6^{-1/2}(Y + iZ)\downarrow - (\frac{2}{3})^{1/2}X\uparrow, \\ |\frac{1}{2}, \frac{1}{2}\rangle &= 3^{-1/2}(Y + iZ)\downarrow + 3^{-1/2}X\uparrow, \end{aligned} \quad (5)$$

and their time-reversed mates. X , Y , and Z are orbital wave functions with the same symmetry as yz , zx , and xy under the operations of the point group. The energies of the three perturbed gaps, as obtained from Eqs. (4) and (5), are, to first order in the stress,²⁰

$$\begin{aligned} \omega(\frac{3}{2}, \frac{3}{2}) &= E_0 + \delta\omega_H + \frac{1}{2}\delta\omega_{100}, \\ \omega(\frac{3}{2}, \frac{1}{2}) &= E_0 + \delta\omega_H - \frac{1}{2}\delta\omega_{100}, \\ \omega(\frac{1}{2}, \frac{1}{2}) &= E_0 + \Delta_0 + \delta\omega_H, \end{aligned} \quad (6)$$

where the hydrostatic shift $\delta\omega_H$ and the shear splitting

¹⁹ B. O. Seraphin and N. Bottka, Phys. Rev. **145**, 628 (1966).

²⁰ F. H. Pollak and M. Cardona, Phys. Rev. **172**, 816 (1968).

$\delta\omega_{100}$ are given by

$$\begin{aligned}\delta\omega_H &= a(S_{11} + 2S_{12})X, \\ \delta\omega_{100} &= 2b(S_{11} - S_{12})X.\end{aligned}\quad (7)$$

X is the magnitude of the [100] stress and S_{ij} are the elastic compliances. A cubic material becomes optically uniaxial under [100] stress. From Eqs. (3), (5), and (6), we obtain for the two components of the tensor $\Delta\epsilon$ in the neighborhood of E_0

$$\begin{aligned}\Delta\epsilon_{11} &\propto (i/3)(\omega - \omega_0)^{-1/2}(\delta\omega_H - \frac{1}{2}\delta\omega_{100}), \\ \Delta\epsilon_{\perp} &\propto (i/3)(\omega - \omega_0)^{-1/2}(\delta\omega_H + \frac{1}{4}\delta\omega_{100}).\end{aligned}\quad (8)$$

In the neighborhood of $E_0 + \Delta_0$, $\Delta\epsilon$ should be given by

$$\Delta\epsilon_{11} = \Delta\epsilon_{\perp} = (i/6)(\omega - \omega_0 - \Delta_0)^{-1/2}\delta\omega_H.\quad (9)$$

From Eqs. (2) and (8), we obtain for the ratio of the piezoreflectance signals at E_0 , with \mathbf{E} parallel and perpendicular to the stress,

$$(\Delta R_{11}/\Delta R_{\perp})_{X \parallel [100]} = (\delta\omega_H - \frac{1}{2}\delta\omega_{100})/(\delta\omega_H + \frac{1}{4}\delta\omega_{100}).\quad (10)$$

Equation (10) remains valid for [111] stress (but not for [110] stress!) provided one replaces $\delta\omega_{100}$ by the corresponding splitting $\delta\omega_{111} = 3^{-1/2}dS_{44}X$. Hence, the ratios $\delta\omega_{100}/\delta\omega_H$ and $\delta\omega_{111}/\delta\omega_H$, and, correspondingly, the ratios b/a and d/a , can be determined from the observed strengths of the piezoreflectance signals for \mathbf{E} parallel and perpendicular to the stress without knowing the magnitude of this stress.

The stress Hamiltonian of a material with wurtzite structure has been given by Pikus.¹⁶ From this Hamiltonian, we find, under the assumption of a stress-independent and isotropic spin-orbit interaction, the energies of the three exciton peaks A, B, and C, which correspond to the E_0 , $E_0 + \Delta_0$ gaps of zinc blende:

$$\begin{aligned}\omega_A &= \omega_A^0 + C_1 e_{zz} + C_2(e_{xx} + e_{yy}) \\ &\quad + C_3 e_{zz} + C_4(e_{xx} + e_{yy}), \\ \omega_B &= \omega_B^0 + C_1 e_{zz} + C_2(e_{xx} + e_{yy}) \\ &\quad + \alpha_+ [C_3 e_{zz} + C_4(e_{xx} + e_{yy})], \\ \omega_C &= \omega_C^0 + C_1 e_{zz} + C_2(e_{xx} + e_{yy}) \\ &\quad + \alpha_- [C_3 e_{zz} + C_4(e_{xx} + e_{yy})].\end{aligned}\quad (11)$$

Because of the small stresses inherent to modulation work, only first-order terms have been kept in Eq. (11). Two extra deformation potentials, C_5 and C_6 , are required to account for nonlinearities due to stress coupling between the various valence-band states. The coefficients α_{\pm} represent the mixing of the orbital states by the spin-orbit interaction. They are given by

$$\alpha_{\pm} = \frac{1}{2} \{ 1 \pm (\Delta_1 - \Delta_2) [(\Delta_1 - \Delta_2)^2 + 8\Delta_2^2]^{-1/2} \},\quad (12)$$

where Δ_1 is the crystal-field splitting of the Γ_1 - Γ_5 orbital states and $\Delta_2/3$ is the relevant matrix element of the spin-orbit interaction. Because of the analogy of the shift represented in Eq. (11) by C_1 and C_2 with the

hydrostatic shift of a zinc-blende-type material, we shall call C_1 and C_2 "hydrostatic" deformation potentials, while C_3 and C_4 will be called "shear" deformation potentials. One should, however, emphasize the fact that, in general, both C_3 and C_4 will contribute to Eq. (11) when a hydrostatic stress is applied.

For stresses along [0001] and [1120], we obtain

$$\begin{aligned}\Delta\omega_A &= \delta\omega_H + \delta\omega_X, \\ \Delta\omega_B &= \delta\omega_H + \alpha_+ \delta\omega_X, \\ \Delta\omega_C &= \delta\omega_H + \alpha_- \delta\omega_X\end{aligned}\quad (13)$$

with

$$\begin{aligned}\delta\omega_H(X \parallel c) &= \delta\omega_{Hc} = (C_1 S_{33} + 2C_2 S_{13})X, \\ \delta\omega_H(X \perp c) &= \delta\omega_{Ha} = 2[C_1 S_{13} + C_2(S_{11} + S_{12})]X, \\ \delta\omega_X(X \parallel c) &= \delta\omega_c = (C_3 S_{33} + 2C_4 S_{13})X, \\ \delta\omega_X(X \perp c) &= \delta\omega_a = 2[C_3 S_{13} + C_4(S_{11} + S_{12})]X.\end{aligned}\quad (14)$$

In Eq. (14), S_{ij} are the elastic compliances and X is the magnitude of the stress. If we again neglect the change in the momentum matrix elements induced by the stress, we obtain the following simple and useful relations:

$$\rho_c = \left(\frac{\Delta R_{\perp}(A)/R_{\perp}'(A)}{\Delta R_{\perp}(B)/R_{\perp}'(B)} \right)_{X \parallel c} = \frac{\delta\omega_{Hc} + \delta\omega_c}{\delta\omega_{Hc} + \alpha_+ \delta\omega_c},\quad (15)$$

$$\rho_a = \left(\frac{\Delta R_{\perp}(A)/R_{\perp}'(A)}{\Delta R_{\perp}(B)/R_{\perp}'(B)} \right)_{X \perp c} = \frac{\delta\omega_{Ha} + \delta\omega_a}{\delta\omega_{Ha} + \alpha_+ \delta\omega_a}.\quad (16)$$

$R'(A)$ and $R'(B)$ are the strengths of the wavelength derivative reflection spectra of the A and B excitons. If we measure $(\Delta R/R)$ for the A and B excitons with light polarized perpendicular to the c axis, and with the stress applied along [0001] (c) and [1120] (a), we can obtain the shear deformation potentials C_3 and C_4 as linear combinations of the hydrostatic deformation potentials C_1 and C_2 , provided the wavelength derivative reflection spectra are also measured. We should say that Eqs. (15) and (16) follow independently of the validity of Eq. (3) for excitons.

B. Exchange Interaction

In the analysis of the stress effects on the excitonic transitions of the wurtzite-type II-VI compounds, we have not considered the two-particle character of these states. Koda and Langer¹⁷ have reported a splitting of the A and B excitons of the wurtzite-type materials considered here produced by the stress. The one-electron Hamiltonian used above to derive the strength of the piezoreflectance signals does not predict any splitting of the Kramers degenerate A or B excitons. In order to explain this splitting, one has to take into account the two-particle character of the exciton. (The Kramers degeneracy of the one-electron states is, in principle, lifted for two-particle exciton states.) By considering the exchange interaction between the electron and the

hole, together with the orbital Hamiltonian of the externally applied stress, it is possible to explain the observed splittings. Akimoto and Hasegawa¹⁸ have solved this problem with a number of simplifying assumptions. They assume that one of the Γ_7 valence bands (C exciton) is very far from the other valence bands (Γ_7 and Γ_9), and also that the forbidden states of the excitons are far removed from those optically allowed. With these approximations, they find the following energies for the A and B allowed excitons:

$$\omega = \omega_0 \pm \frac{1}{2} \Delta \pm \frac{1}{2} \delta, \quad (17)$$

where ω is the energy of the four split valence bands, δ is the magnitude of the exchange-induced splitting, and Δ represents the difference between the centers of gravity of the two split levels in each exciton. To first order in the strain, δ and Δ are of the form¹⁸

$$\begin{aligned} \delta &= [4\gamma P(0)J\Omega/\Delta_0]D_u X, \\ \Delta &= \Delta_0 - (1-\gamma)\{1 - 4\gamma[JP(0)/\Delta_0]^2\}^{1/2}D_u X, \end{aligned} \quad (18)$$

where X is the applied stress, D_u is an appropriate deformation potential, $P(0)$ is the amplitude of the exciton-envelope function at the origin, Δ_0 is the energy difference between the A-B excitons with no stress applied, J is the exchange integral, and γ is a parameter of the quasicubic model²¹ that gives the mixing of the cubic states produced by the hexagonal crystal field. For the A-B interaction, γ is given by the α_+ of Eq. (12). Ω is the volume of the primitive unit cell. The results of Eq. (18) should be accurate for CdSe and ZnO, but not for CdS because of the relative proximity of the two Γ_7 states. Moreover, a possible hydrostatic shift of all the peaks, corresponding to the deformation potentials C_1 and C_2 , is not included in Eq. (17).

The complete exchange-stress Hamiltonian for the A, B, C peaks has been given by Koda *et al.*²² From this Hamiltonian, we find, under the assumption of isotropic spin-orbit interaction, and to first order in X and J ,

$$\begin{aligned} \omega_A^\pm &= \omega_A^0 + \delta\omega_{Ha} + \delta\omega_a \\ &\pm \left(\frac{\alpha_+^2}{\omega_B^0 - \omega_A^0} + \frac{\alpha_-^2}{\omega_C^0 - \omega_A^0} \right) \delta_J \delta\omega_J, \quad (19) \\ \omega_B^\pm &= \omega_B^0 + \delta\omega_{Ha} + \alpha_+ \delta\omega_a \\ &\pm [\alpha_+^2/(\omega_B^0 - \omega_A^0)] \delta_J \delta\omega_J, \end{aligned}$$

where $\delta\omega_J$ and δ_J are

$$\begin{aligned} \delta\omega_J &= 4C_5(S_{11} - S_{12})X, \\ \delta_J &= P(0)\Omega J. \end{aligned} \quad (20)$$

²¹ J. J. Hopfield, *J. Phys. Chem. Solids* **15**, 97 (1960).
²² T. Koda, D. W. Langer, and R. N. Euwema, in *Proceedings of the Ninth International Conference on the Physics of Semiconductors*, edited by S. M. Rytvkin (Nauka Publishing House, Leningrad, 1968), p. 242. The C_5 of this work differs from ours by a factor of 2 because of its definition. We have consistently used the definition of Ref. 29.

The energy shifts $\delta\omega_{Ha}$ and $\delta\omega_a$ have been defined in Eq. (14). C_5 is a deformation potential¹⁶ which corresponds to the Γ_6 irreducible component of the stress tensor. Optical transitions to the four states ω_A^\pm , ω_B^\pm are completely polarized parallel or perpendicular to the direction of the stress, a fact that simplifies its observation. The discussion can be easily extended to the C excitons; we do not do it since in our experiment they have never been observed with sufficient strength to obtain information on the exchange splitting. From Eqs. (16) and (19), we find

$$\begin{aligned} \left(\frac{\Delta R_1(A)}{\Delta R_{11}(A)} \right)_{X \perp c} &= \frac{\delta\omega_{Ha} + \delta\omega_a + \beta_A \delta_J \delta\omega_J}{\delta\omega_{Ha} + \delta\omega_a - \beta_A \delta_J \delta\omega_J}, \\ \left(\frac{\Delta R_1(B)}{\Delta R_{11}(B)} \right)_{X \perp c} &= \frac{\delta\omega_{Ha} + \alpha_+ \delta\omega_a + \beta_B \delta_J \delta\omega_J}{\delta\omega_{Ha} + \alpha_+ \delta\omega_a - \beta_B \delta_J \delta\omega_J}, \end{aligned} \quad (21)$$

where

$$\begin{aligned} \beta_A &= \alpha_+^2/(\omega_B^0 - \omega_A^0) + \alpha_-^2/(\omega_C^0 - \omega_A^0), \\ \beta_B &= \alpha_+^2/(\omega_B^0 - \omega_A^0). \end{aligned}$$

Hence, if we applied the stress along the $[11\bar{2}0]$ direction and measure the ratio of the signals perpendicular and parallel to the direction of the stress, we can obtain information about the exchange-interaction parameter, provided we know the ratio of the shear to the hydrostatic deformation potential $\delta\omega_a/\delta\omega_{Ha}$, which can be obtained from Eq. (16), and the ratio $\delta\omega_J/\delta\omega_{Ha}$, which can be obtained if the deformation potentials C_1 , C_2 , and C_5 are known.

C. Ionic Contribution to the Deformation Potentials

In a previous paper,¹⁵ we have proposed a point-ion model to account for the observed values of the deformation potentials of the alkali halides. Here we shall extend this treatment to the III-V and II-VI compounds with zinc-blende structure. The difference in the deformation potentials between the covalent materials (Ge) and the partially ionic III-V (GaAs) and II-VI (ZnSe) compounds will be explained as due to the change in the Coulomb interaction between the displaced ions in the distorted lattice and the anisotropic p -like wave functions of the valence bands.

For either a $[100]$ or a $[111]$ stress, the stress-induced anisotropy of the Coulomb potential of the ions splits the orbital p -wave functions of the valence band into a doublet and a singlet. The matrix element of the electric-dipole transitions between the valence orbital doublet and the s -like conduction band is allowed for polarization perpendicular to the stress, while for the valence singlet it is allowed for the parallel polarization. We have simplified the calculations by replacing the charge density of the p orbitals by two charges displaced with respect to the atomic site by $\pm r_0$ along the symmetry axis of the orbital. The displacement r_0 is chosen as the point where the charge density of the atomic orbital has

TABLE I. Contributions from the Coulomb potential of first and second neighbors to the energy shift $\Delta\omega$ of the singlet component of the Γ_{15} state of zinc blende for stress along the [100] and [111] directions.

$\Delta\omega$	[100] stress	[111] stress
First neighbors	$-49\left(\frac{r_0}{a}\right)^2 \frac{qe^2}{a}\epsilon$	$-49\left(\frac{r_0}{a}\right)^2 \frac{qe^2}{a}\epsilon$
Second neighbors	$+13\left(\frac{r_0}{a}\right)^2 \frac{qe^2}{a}\epsilon$	$-13\left(\frac{r_0}{a}\right)^2 \frac{qe^2}{a}\epsilon$

its maximum. We have used as wave functions the atomic wave functions of Herman and Skillman.²³ It has been shown previously¹⁵ that this crude point-ion model gives results which differ from those obtained with the full atomic wave function by less than a factor of 2.

With these approximations, we have calculated the contribution to the ionic part of the deformation potentials b and d of the zinc-blende structure due to the interaction of the charges with the first and second neighbors. For stress along the [100] and [111] directions,

$$\Delta\omega = -e^2q \left[\sum_k \left(\frac{1}{|r_k' \pm r_0|} - \frac{1}{|r_k \pm r_0|} \right) - \sum_p \left(\frac{1}{|r_l' \pm r_0|} - \frac{1}{|r_l \pm r_0|} \right) \right], \quad (22)$$

where $\Delta\omega$ is the change in energy of the singlet state produced by the applied stress, q is the ionic charge in e units, r_k and r_l are the positions in the unstrained crystal of the first and second neighbors, respectively, and r_k' and r_l' are the positions of these neighbors in the strained crystal.

Symmetry requires the position of the atoms within a given sublattice to scale like the macroscopic strain

$$r_{li}' = e_{ij}r_{lj} + r_{li}. \quad (23)$$

For a [100] stress, and in the germanium lattice (not zinc blende), symmetry also forces the two lattices to displace with respect to each other like the macroscopic strain

$$r_{ki}' = e_{ij}r_{kj} + r_{ki}. \quad (24)$$

This result should not hold strictly for zinc blende; an additional internal coordinate is necessary to describe the unit cell of the material stressed along [100]. In the absence of experimental information about this parameter, we shall operate under the assumption that the relative shift of the two sublattices of zinc blende is given by Eq. (24). As is well known, the crystal poten-

tial of a zinc-blende-type material is equivalent to that of a germanium type plus a small antisymmetric perturbation.

For a stress along [111], an additional internal coordinate is necessary even for germanium lattices.²⁴ X-ray measurements²⁵ on germanium have shown that the separation along [111] between the two sublattices remains practically unchanged under [111] stress: The covalent bond is very incompressible. We shall perform our calculation under these assumptions. We have also performed calculations under the opposite assumption: a sublattice shift given by the macroscopic strain [Eq. (24)]. In this case, the agreement of the calculated contributions to the deformation potentials with the experimental results is poor. This fact may be interpreted as further evidence for the incompressibility of the covalent bond. The results obtained for the ionic contribution to the energy shift $\Delta\omega$ of the singlet are shown in Table I. ϵ is the pure shear strain along the stress axis and a is the lattice constant. With a typical value of $r_0 \approx a_0/8$ (a_0 is the lattice constant) (i.e., the value obtained for GaAs from Ref. 23), we obtain for the ionic contribution to the deformation potentials

$$\begin{aligned} \Delta d &= -1.4q \text{ eV}, \\ \Delta b &= -0.47q \text{ eV}. \end{aligned} \quad (25)$$

There is some uncertainty as to what values to use for the ionic charge q of these compounds. For the sake of comparison, we use the values of q obtained from the infrared reststrahlen spectra.²⁶ Typically, $q = +0.5$ for the III-V compounds and $q = +0.8$ for the II-VI compounds. With these values of q , Eq. (25) yields:

for III-V compounds,

$$\Delta b = -0.23 \text{ eV}, \quad \Delta d = -0.69 \text{ eV}, \quad (26)$$

for II-VI compounds,

$$\Delta b = -0.38 \text{ eV}, \quad \Delta d = -1.11 \text{ eV}.$$

We have also made a rough calculation of the contribution of the third nearest neighbors to b and d and shown that it should be negligible within the uncertainty of the model.

Finally, we should point out that the results in Table I can also be used to estimate the deformation potentials of the covalent materials. If we use a charge $q = +4$ for both first and second neighbors (we must reverse the sign of ΔE for the second neighbors), we obtain (for $r_0 = a_0/8$), $b = -3.1$ eV and $d = -3.3$ eV, which are not too far from the experimental values for germanium ($b = -2.6$ and $d = -4.7$).²⁰

²⁴ I. Goroff and L. Kleinman, Phys. Rev. **132**, 1080 (1963).

²⁵ A. Segmüller, Phys. Letters **4**, 227 (1963).

²⁶ S. S. Mitra, in *Optical Properties of Solids*, edited by S. Nudelman and S. S. Mitra (Plenum Press, Inc., New York, 1969), pp. 414-417.

²³ F. Herman and S. Skillman, *Atomic Structure Calculations* (Prentice-Hall, Inc., Englewood Cliffs, N. J., 1963).

III. EXPERIMENT

A. Optical Equipment

Light from either a high-pressure 500-W xenon arc (uv) or a 650-W quartz-iodine tungsten filament lamp (visible and infrared) was focused on the entrance slit of a 580-mm Model-14 Perkin-Elmer monochromator. The monochromatic light was linearly polarized by means of suitable polarizers, focused on the sample, reflected at near-normal incidence, and refocused on either an EMI 6255S or a Dumont 6911 photomultiplier for the ultraviolet visible and near infrared, respectively. A PbS Kodak Ektron cell was used for wavelengths longer than $1\ \mu$. Slit widths corresponding to spectral resolutions ranging from $1\ \text{\AA}$ in the ultraviolet to $20\ \text{\AA}$ in the infrared were used.

B. Electronic Equipment

The experimental setup was similar to that used for electroreflectance measurements.² The photomultiplier signal contains a component proportional to the reflectance of the sample R and an ac component proportional to the modulated change in the reflectance ΔR produced by the periodic strain in the sample. The ac signal was detected with a Princeton Applied Research HR8 lock-in amplifier, the output of which was plotted as a function of wavelength with a strip-chart recorder. The output was kept constant at 200 mV by varying the high voltage applied to the photomultiplier with a servo. The signal so obtained is, therefore, proportional to $\Delta R/R$. For the measurements in the infrared with a PbS photoconductive cell as detector, the scheme given above cannot be used. In this case, a portion of the incident light is mechanically chopped at 80 Hz. The signal at 80 Hz, proportional to R , and the signal at the modulation frequency, proportional to ΔR , are separately detected with two lock-in amplifiers. Both outputs are fed to an electronic ratiometer, and the ratio is plotted with a recorder as a function of wavelength.

TABLE II. List of samples and surface preparations used for the piezoreflectance measurements.

Sample	Carrier concentration (cm^{-3})	Type	Surface preparation
Ge	10^{14}	<i>p</i>	etched $\text{HNO}_3:\text{HF}:\text{CH}_3\text{COOH}$ 25:15:15
GaAs	10^{15}	<i>n</i>	etched $\text{Br}_2:\text{CH}_3\text{OH}$ 1:100
GaSb	10^{16}	<i>n</i>	etched $\text{Br}_2:\text{CH}_3\text{OH}$ 1:500
InP	10^{16}	<i>n</i>	etched $\text{Br}_2:\text{CH}_3\text{OH}$ 1:100
ZnS	unknown	<i>n</i>	etched $\text{H}_2\text{SO}_4:\text{KMnO}_4$ 50:1 cleaved
CdTe	10^{15}	<i>n</i>	etched $\text{H}_2\text{O}:\text{HNO}_3:\text{K}_2\text{Cr}_2\text{O}_7$ 10:10:4
CdS	unknown	<i>n</i>	surface of growth from vapor etched $\text{H}_2\text{SO}_4:\text{KMnO}_4$ 50:1
CdSe	unknown	<i>n</i>	cleaved etched $\text{H}_2\text{SO}_4:\text{KMnO}_4$ 50:1
ZnO	unknown	<i>n</i>	cleaved etched H_3PO_4

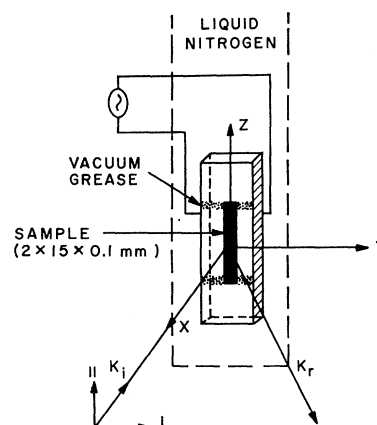


FIG. 1. Details of the transducer modulator used for piezoreflectance measurements.

The transducer, a PZT bar of approximate dimensions $30 \times 10 \times 5\ \text{mm}$, is driven typically at 200 Hz with voltages ranging from 500 to 1400 V obtained by suitable power amplification of the output of the reference channel of the lock-in amplifier.

C. Sample Preparation and Mounting

The samples were oriented by x-ray diffraction to within 1° . In order to have the largest possible stress and a uniform distribution of it in the sample, the thickness of the sample was kept below $150\ \mu$; the length and width were typically of the order of 15 and 1 mm, respectively. The back surface of the sample was kept rough from the lapping process to minimize spurious signals due to back reflections. The reflecting front surface was cleaved whenever possible. For materials which do not cleave easily, or for faces other than that of cleavage, the reflecting surface was mechanically polished with $0.3\text{-}\mu$ alumina powder and chemically etched. All the relevant information about the samples and the methods of preparation is given in Table II.

The samples were mounted on the transducer as shown in Fig. 1. We used a small amount of silicone vacuum grease at the ends of the sample to bond it to the transducer. The use of grease has the advantage over other methods of supporting the samples that when the sample is cooled most of the strain produced by the differential compression between itself and the transducer is released by the grease.

For the particular shape of the samples used, with the mounting procedure just described, the stress is expected to be uniform and along the length of the sample, at least in its central part where the probing light is focused. The transducer was mounted in a brass frame and supported with small nylon screws; the modulating power was applied to the transducer by means of copper leads attached to the transducer electrodes with silver paint. The frame was mounted inside a quartz Dewar

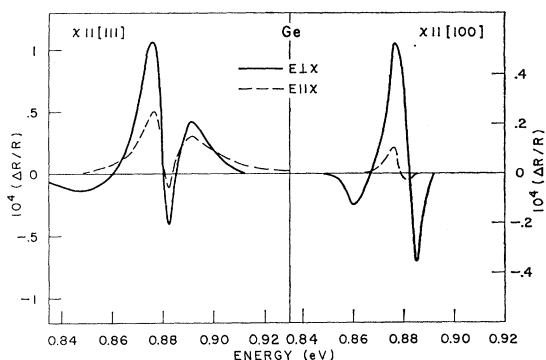


FIG. 2. Piezoreflectance spectra of Ge for stress applied along the [111] and [100] directions at 77°K.

and cooled by immersion in liquid nitrogen. Bubbles in the liquid nitrogen can be avoided by keeping the Dewar and the liquid nitrogen meticulously clean. From the size of the signals observed the stress applied to the sample was estimated to be of the order of 10^6 dyn cm^{-2} .

IV. RESULTS

A. Zinc-Blende Materials

In Fig. 2, we show the piezoreflectance spectrum of the direct gap of Ge at 77°K with the stress applied along the [100] and the [111] directions. Data are presented for light polarized parallel and perpendicular to the direction of the stress. These results are very similar to those at 300°K reported by Balslev⁸ for stress along the [111] direction.

Figure 3 shows similar results for GaAs. For both directions of the stress, there is a peak at 1.482 eV which seems due to reflection on the back of the sample. To test this assumption, the sample oriented along the [111] direction was polished also in the back face, and in this case the alleged back reflection signal becomes 10 times larger than the piezoreflectance signal. The spectra for the [111] stress are very similar to previous results by Balslev,⁸ except for a small photon energy

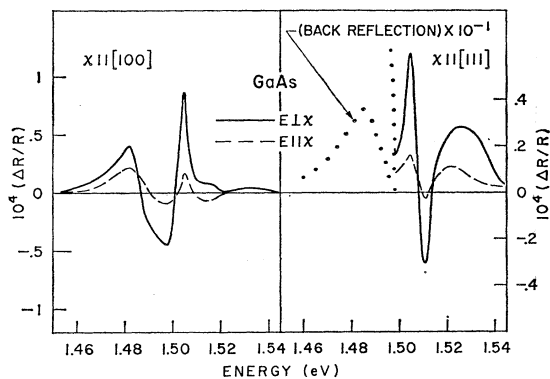


FIG. 3. Piezoreflectance spectra of GaAs for stress applied along the [100] and [111] directions at 77°K.

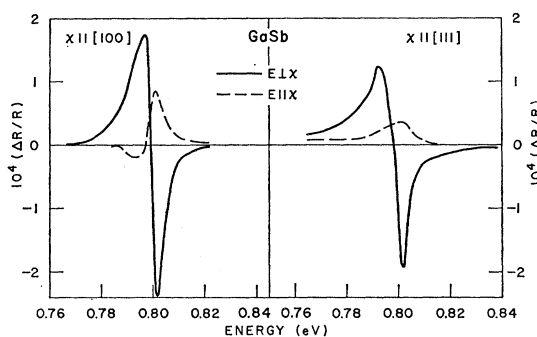


FIG. 4. Piezoreflectance spectra of GaSb for stress applied along the [100] and [111] directions at 77°K.

shift (Balslev's measurements were made at 100°K with the sample above the liquid-nitrogen level).

Figure 4 shows analogous piezoreflectance results for GaSb. In this material, the signal for light polarized parallel to the direction of the stress has reversed its direction. This implies a larger value of the ratio of shear to hydrostatic deformation potentials; one of the split gaps $[(\frac{3}{2}, \frac{3}{2})]$ decreases in energy under a compressive stress while the other $[(\frac{3}{2}, \frac{1}{2})]$ increases. The analogous piezoreflectance spectra of InP are shown in Fig. 5. The spectrum for $X \parallel [100]$ has, other than the peak due to the direct edge at 1.41 eV, a strong peak (actually a doublet) at 1.385 eV. This peak has been reported previously,² and, while the exact mechanism which causes it is not known, it is believed due to an impurity level. The strong polarization dependence of this transition should be helpful in identifying its mechanism. For X parallel to [100], the impurity structure is absent; the sample was obtained from a different batch of InP. The direct-edge peaks for [100] stress show opposite sign for the two polarization directions. For [111] stress, the signal observed with $E \parallel X$ is practically zero and has not been represented.

Figure 6 shows the piezoreflectance spectra of ZnS. With the stress along [111] the signals for parallel and perpendicular polarizations have opposite signs. The material used in these measurements was natural

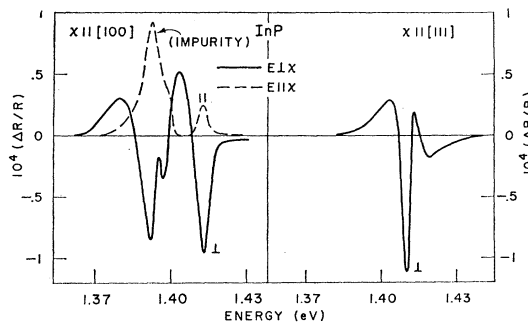


FIG. 5. Piezoreflectance spectra of InP for stress applied along the [100] and [111] directions at 77°K.

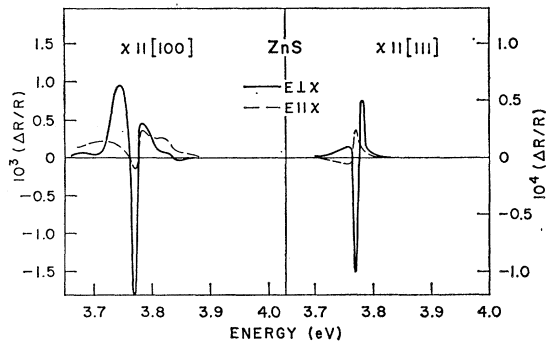


FIG. 6. Piezoreflectance spectra of ZnS for stress applied along the $[100]$ and $[111]$ directions at 77°K .

sphalerite.²⁷ Similar results were obtained with synthetic nearly cubic ZnS for $[100]$ stress (no measurements were performed with synthetic ZnS for $[111]$ stress).

The piezoreflectance spectra of CdTe are shown in Fig. 7. In this material, a sign reversal of the signal with polarization is observed for both $[100]$ and $[111]$ stress directions.

B. Wurtzite Materials

Figure 8 shows the piezoreflectance results for CdSe for the stress applied along the $[0001]$ and the $[11\bar{2}0]$ directions with light polarized parallel and perpendicular to the direction of the c axis ($[0001]$ direction). For all data in Fig. 8, the direction of propagation of the light (\mathbf{K}) was perpendicular to the c axis. The peaks at 1.840 and 1.815 eV correspond to the A and B excitons, and the energy difference between them agrees well with previous results.¹⁷ The peak corresponding to the A exciton has opposite sign for $[0001]$ and for $[11\bar{2}0]$ stress. The sign of the energy shift with stress derived from these results agrees well with that obtained from reflectivity measurement under large static stress.¹⁷

Figure 9 shows similar spectra for CdS, also with the stress applied along the $[0001]$ and the $[11\bar{2}0]$ directions and with \mathbf{K} perpendicular to c . The three excitons

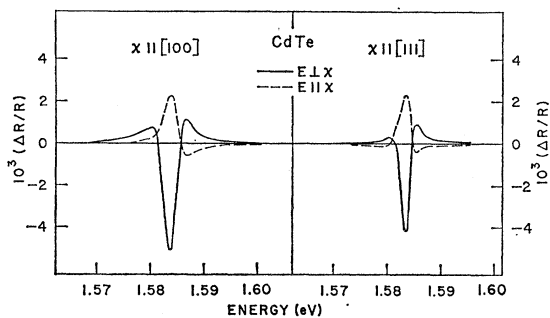


FIG. 7. Piezoreflectance spectra of CdTe for stress applied along the $[100]$ and $[111]$ directions at 77°K .

²⁷ Juan Montal, Villafranca del Panades, Spain (private communication).

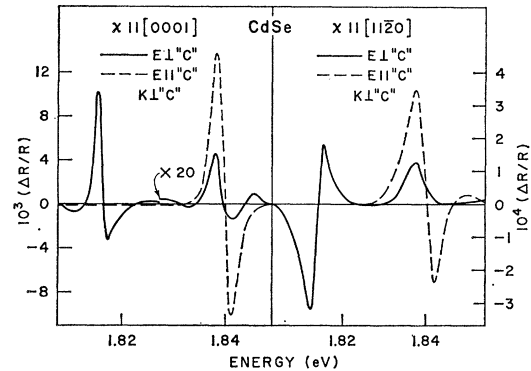


FIG. 8. Piezoreflectance spectra of CdSe for stress applied along the $[0001]$ and $[11\bar{2}0]$ directions at 77°K .

A, B, and C can be seen in the piezoreflectance spectrum at 2.544, 2.558, and 2.615 eV, respectively. The splittings of the excitons A-B and A-C, 14 and 71 meV, respectively, agree well with previous results.²⁸ The piezoreflectance signal due to both A and B excitons has for $[0001]$ stress a sign opposite to that for $[11\bar{2}0]$ stress. This result seems to disagree with the stress dependence of peak positions derived from previous reflectance measurements under high static stress²⁹; according to these measurements, the signal from the exciton B should not change sign. One should point out, however, that static stress measurements do not yield the slope of peak energies at zero stress as accurately as modulated stress measurements. The data for $[11\bar{2}0]$ stress in Fig. 9 show that, if the incidence is not very close to normal, the A exciton is not strictly forbidden for light polarized with \mathbf{E} parallel to c (dashed line).

Figures 10(a) and 10(b) show piezoreflectance spectra of CdSe and CdS, respectively, for the stress applied along the $[11\bar{2}0]$ and the c axis parallel to the direction of propagation of the light. This figure shows a clear polarization dependence of the peak-to-peak intensity

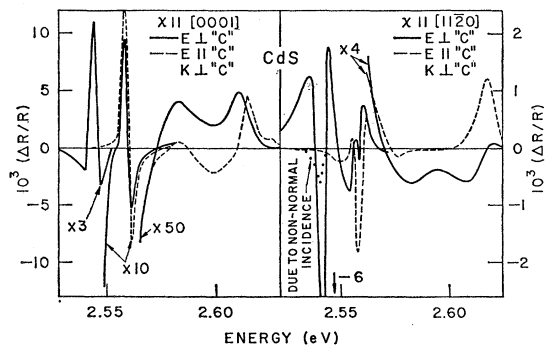


FIG. 9. Piezoreflectance spectra of CdS for stress applied along the $[0001]$ and $[11\bar{2}0]$ directions at 77°K .

²⁸ J. J. Hopfield and D. G. Thomas, Phys. Rev. **122**, 35 (1961).
²⁹ J. E. Rowe, M. Cardona, and F. H. Pollak, in *Proceedings of the International Conference on II-VI Semiconductors Compounds, Providence, 1967*, edited by D. G. Thomas (W. A. Benjamin, Inc., New York, 1967), p. 112.

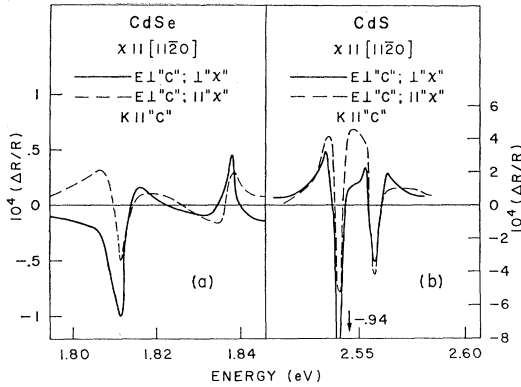


FIG. 10. Piezoreflectance spectra at 77°K for stress applied along the $[11\bar{2}0]$ direction and $\mathbf{K} \parallel c$. (a) CdSe; (b) CdS.

of the signal, stronger for CdS than for CdSe. This effect could have been predicted from measurements of the exchange splitting of the excitons under high static stress by Koda *et al.*^{17,22}

Figure 11 shows the piezoreflectance spectra of ZnO for the three stress and polarization configurations discussed above. Figure 11(a) corresponds to a $[0001]$ stress and $\mathbf{K} \perp c$, Fig. 11(b) to $[11\bar{2}0]$ stress and $\mathbf{K} \parallel c$, and Fig. 11(c) to $[11\bar{2}0]$ stress and $\mathbf{K} \perp c$. The three peaks at 3.367, 3.380, and 3.422 eV correspond to the A, B, and C excitons, respectively. The positions of these three peaks agree very well with previous measurements using differential techniques.⁵ The energy separation of the A and B excitons agrees well with that found from differential measurements,⁵ but it is twice as large as the one obtained from static reflectivity measurements.^{30,31} This apparent discrepancy can be attributed to the fact that the A-B splitting is about the same as the width of the peaks, while the width of peak A is much smaller than that of peak B. In the differential spectra, the peaks correspond to the points

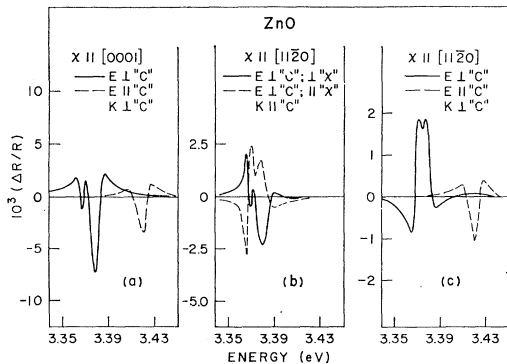


FIG. 11. Piezoreflectance spectra of ZnO at 77°K. (a) stress applied along the $[0001]$ direction; (b) stress along $[11\bar{2}0]$, $\mathbf{K} \parallel c$; (c) stress along $[11\bar{2}0]$, $\mathbf{K} \perp c$.

³⁰ D. G. Thomas, *J. Phys. Chem. Solids* **15**, 86 (1960).

³¹ Y. Park, C. Litton, T. Collins, and D. C. Reynolds, *Phys. Rev.* **143**, 512 (1966).

TABLE III. Values of the parameters used in the calculation of the shear deformation potentials of the zinc-blende materials.

	$10^{12}S_{11}$ ($\frac{\text{cm}^2}{\text{dyn}}$)	$10^{12}S_{12}$ ($\frac{\text{cm}^2}{\text{dyn}}$)	$10^{12}S_{44}$ ($\frac{\text{cm}^2}{\text{dyn}}$)	$10^6 \frac{\partial E_g}{\partial P}$ (eV/bar)
Ge ^a	0.98	-0.27	1.49	13 ^b
GaAs ^c	1.16	-0.37	1.67	11 ^b
GaSb ^a	1.58	-0.50	2.31	14 ^b
InP ^d	1.74	-0.61	2.24	8.5 ^b
ZnS ^a	1.97	-0.76	2.36	5.7 ^e
CdTe ^f	4.27	-1.73	5	11.4 ^f

^a H. B. Huntington, in *Solid State Physics*, edited by F. Seitz and D. Turnbull (Academic Press Inc., New York, 1958), Vol. 5.

^b R. Zallen and W. Paul, *Phys. Rev.* **155**, 703 (1967).

^c J. R. Drabble, in *Semiconductors and Semimetals*, edited by R. K. Willardson and A. C. Beer (Academic Press Inc., New York, 1966), Vol. 2.

^d The elastic constants of InP have been interpolated from the known values for other III-V compounds as a function of the lattice constant.

^e A. L. Edwards, J. E. Slykhouse, and H. G. Drickamer, *J. Phys. Chem. Solids* **11**, 140 (1959).

^f D. G. Thomas, *J. Appl. Phys.* **32S**, 2298 (1961).

of maximum slope in the reflectivity and not to the static-reflectivity maxima. Under the conditions described above, large differences between the splitting as measured at the points of the maximum slope or at the peaks of the reflection spectrum should occur. For ZnO, the reflectivity maxima correspond rather closely to the maxima in ϵ_i and, thus, to the exciton energies.³¹ It should also be noticed that in spectrographic measurements of the reflection spectrum, where the positions of the peaks were defined as the minimum of the reflectivity,¹⁷ a large A-B splitting was found, as expected from the argument above. For the stress along $[11\bar{2}0]$ and $\mathbf{K} \parallel c$ there is a very strong polarization dependence of the signal, much stronger than for either CdSe or CdS. This polarization dependence parallels the splitting of the A and B peaks found from the reflection spectrum under static stress.¹⁷

V. DISCUSSION

A. Zinc-Blende Materials

Using Eq. (10) and the known values of the hydrostatic deformation potentials and elastic constants of these materials (see Table III), we obtained the values of the shear deformation potentials b and d . These results, together with values obtained previously with static stress techniques, have been listed in Table IV. We can see that for Ge, GaAs, and CdTe, materials for which there are independent values of b and d obtained

TABLE IV. Deformation potentials b and d obtained from the piezoreflectance measurements and the parameters of Table III.

	Ge	GaAs	GaSb	InP	ZnS	CdTe
b^a (eV)	-2.8	-1.75	-3.3	-1.55	-0.53	-1.1
	-2.6 ^b	-2.0 ^b				-1.18 ^c
d^a (eV)	-4.95	-5.55	-8.35	-4.4	-3.7	-5.45
	-4.7 ^b	-6.0 ^b				-4.84 ^c

^a The values b and d have an uncertainty of $\pm 20\%$ which includes a 10% uncertainty in the values of a .

^b See Ref. 20.

^c D. G. Thomas, *J. Appl. Phys.* **32S**, 2298 (1961).

from static stress measurements, good agreement is found; these values differ from ours by less than 10%. There are no independent values of b and d for ZnS, GaSb, and InP to compare with ours. In Table V, we have listed the known values of $\eta = d/\sqrt{3}b$, that is, the ratio of the splitting for a uniaxial strain along [111] to the splitting for a uniaxial strain of the same magnitude along [100] for all measured zinc-blende materials. This Table V shows that there is a monotonic increase in this ratio from Ge and Si (covalent materials, $\eta = 1.06$ and 1.32, respectively) to the III-V compounds ($\eta = 1.42$ for InSb; $\eta = 1.82$ for GaAs) to the more ionic II-VI compounds CdTe ($\eta = 2.8$) and ZnS ($\eta = 4.4$).

This behavior can be qualitatively explained with the results obtained from Eq. (26) and Table II. If we take the b and d values of silicon as representative for the covalent (group IV) materials, we find η ratios of 1.63 and 1.86 for the III-V and II-VI compounds, respectively. If we use the b and d values of germanium, we find 1.20 and 1.34 for the III-V and II-VI compounds, respectively. These values represent well the experimental trend of η presented in Table V. If we try to extrapolate this procedure to the I-VII compounds with zinc-blende structure, we should obtain even larger values of η . No experimental values of b and d are available for these materials (CuCl, CuBr, CuI, AgI). The alkali halides, also I-VII compounds, crystallize in either the NaCl or the CsCl structure. Calculations similar to those described above predict different sign for the ionic contribution to b and d in these materials. This sign reversal has been observed experimentally.¹⁵

B. Wurtzite Materials

For these materials, we can get, using Eqs. (15) and (16),³² the ratio of the shear deformation potentials C_3 and C_4 to the hydrostatic deformation potentials C_1 and C_2 :

$$U_c = \frac{\delta\omega_c}{\delta\omega_{Hc}} = \frac{C_3 S_{33} + 2C_4 S_{13}}{C_1 S_{33} + 2C_2 S_{13}} = -\frac{1 - \rho_c}{1 - \alpha_+ \rho_c},$$

$$U_a = \frac{\delta\omega_a}{\delta\omega_{Ha}} = \frac{C_3 S_{13} + C_4 (S_{11} + S_{12})}{C_1 S_{13} + C_2 (S_{11} + S_{12})} = -\frac{1 - \rho_a}{1 - \alpha_+ \rho_a}.$$

The expression for U_a has been obtained from Eq. (16). As shown earlier, this equation must be modified so as to include exchange interaction. Nevertheless, if we consider the experimental configuration in which the stress is applied along the [1120] direction and \mathbf{K} is parallel to c and take the average of the signals

³² The values of R' , i.e., the strength of the wavelength derivative reflection spectra of the A, B, and C excitons, was obtained with the system described by M. Cardona, in *Proceedings of the Ninth International Conference of the Physics of Semiconductors*, edited by S. M. Ryvkin (Nauka Publishing House, Leningrad, 1968), p. 365. The values of $\Delta R/R$, i.e., the strength of the piezoreflectance spectra of the A, B, and C excitons, was obtained from Figs. 9–11 as the average peak-to-peak value.

TABLE V. Survey of known values of the deformation potentials b and d of materials with zinc-blende and diamond structure. Also, ratio η of valence-bands splitting for the same strain along [111] and [100].

	b (eV)	d (eV)	$\eta = d/\sqrt{3}b$
Sj ^a	-1.36	-3.10	1.32
Ge	-2.8	-4.95	1.06
GaAs	-1.75	-5.55	1.82
GaSb	-3.3	-8.35	1.48
GaP ^b	-1.4	-4.0	1.66
InSb ^c	-2.0	-4.9	1.42
InP	-1.55	-4.4	1.64
AlSb ^d	-1.34	-4.2	1.80
ZnS	-0.53	-3.7	4.10
CdTe	-1.1	-5.45	2.8

^a J. Hensel and G. Feher, Phys. Rev. **129**, 1041 (1963).
^b I. Balslev, Proc. Phys. Soc. Japan Suppl. **21**, 101 (1966).
^c F. H. Pollak and J. Halpern, Bull. Am. Phys. Soc. **14**, 433 (1968).
^d M. Cardona, L. D. Laude, and F. H. Pollak, Bull. Am. Phys. Soc. **14**, 428 (1968).

at each peak for the light polarized parallel and perpendicular to the direction of the stress, the effect of exchange cancels out, as shown by Eq. (19), and Eq. (16) remains valid for these averages. Table VI lists the values obtained for U_c and U_a together with the values of α_+ used for their evaluation from our experimental data. We have also listed in this Table the values of U_c and U_a obtained from measurements under static stress.^{29,33,34} For CdSe, there is good agreement between our values of U_c and U_a and the static stress values. For CdS, we find good agreement for U_c but not for U_a . This corresponds to the already mentioned fact that the B exciton moves to lower energies with small compressions, in contrast to the results found with large static stress.²⁹

For ZnO, Eqs. (15) and (16) do not yield any information since $\alpha_+ \simeq 1$; the A and B excitons move very much in the same way with the stress. It is possible, however, to get information about U_c by comparing the intensities of the B and C excitons. Table VI shows good agreement between our results and those obtained from previous measurements under large static stress.³³ Because of the strong exchange interaction in ZnO, the procedure used to obtain U_a , i.e., to average the strength

TABLE VI. Values of U_a and U_c obtained from piezoreflectance measurements for CdS, CdSe, and ZnO.

	CdSe	CdS	ZnO
U_c	-3.3 (± 0.3)	-4.4 (± 0.4)	1.4 (± 0.1)
	-3.2 ^a	-4.5 ^b	1.26 ^c
U_a	-1.2 (± 0.2)	1 (± 0.3)	
	-1.4 ^a	-1.1 ^b	-0.73 ^c
α_+	0.38 ^d	0.54 ^d	1 ^e

^a See Ref. 34.
^b See Ref. 29.
^c See Ref. 33.
^d Our measurements.
^e See Ref. 31.

³³ J. E. Rowe, M. Cardona, and F. H. Pollak, Solid State Commun. **6**, 239 (1969). There is a computational error in this paper. The correct values of the deformation potentials are those in Table VII.

³⁴ J. E. Rowe (private communication).

TABLE VII. Values for the exchange splittings δ_J and the exchange integral J obtained from piezoreflectance measurements for CdS, CdSe, and ZnO, together with parameters used in their calculation.

	CdSe		CdS		ZnO	
	A	B	A	B	A	B
Exciton						
δ_J (meV)	2.1	1.9	7.6	7.2	1.6	3.2
	-0.16 ^a		2.2 ^a		6.6 ^a	
J (eV)	2.6	2.4	3.3	3.1	0.28	0.56
C_1 (eV)	-1 ^b		-1.7 ^c		-3.9 ^d	
C_2 (eV)	-4.1 ^b		-3.7 ^c		-4.0 ^d	
C_3 (eV)	-4.2 ^b		-2.7 ^c		-1.2 ^d	
C_4 (eV)	-1.9 ^b		1.5 ^c		0.94 ^d	
C_5 (eV)	1.2 ^b		0.58 ^c		0.62 ^d	
a_{ex} (Å)	36		24		14	
$10^{12}S_{11}$ ($\frac{\text{cm}^2}{\text{dyn}}$)	2.34 ^e		2.07 ^e		0.79 ^f	
$10^{12}S_{12}$ ($\frac{\text{cm}^2}{\text{dyn}}$)	-1.12 ^e		-0.99 ^e		-0.34 ^f	
$10^{12}S_{13}$ ($\frac{\text{cm}^2}{\text{dyn}}$)	-0.57 ^e		-0.58 ^e		-0.22 ^f	
$10^{12}S_{33}$ ($\frac{\text{cm}^2}{\text{dyn}}$)	1.73 ^e		1.69 ^e		0.69 ^f	

^a See Ref. 22.

^b See Ref. 34.

^c See Ref. 29.

^d See Ref. 33.

^e T. B. Bateman, J. Appl. Phys. 33, 3309 (1962).

^f D. Berlincourt, H. Jaffe, and L. R. Shiozawa, Phys. Rev. 129, 1009 (1963).

of the signals for light polarized parallel and perpendicular to the direction of the stress, is no longer good; the small average value is of the order of the error. Hence, we will not attempt to obtain U_a for this material.

From our measurements it is also possible to obtain information about the exchange interaction. Using Eq. (21) and the results of Figs. 10(a), 10(b), and 11(b), we can find values for δ_J and J ; these values are listed in Table VII. In order to obtain these values, it is necessary to use results from other independent measurements; the deformation potentials C_1 , C_2 , C_3 , C_4 , and C_5 were taken from Refs. 29, 33, and 34. The exciton radii were calculated using average values of the dielectric constant and the conduction-band mass (see Table VII). The values of δ_J for these materials obtained from static stress measurements are also listed in Table VII. The values of J reported for the alkali halides³⁵ between 1 and 5 eV are in reasonable accord with the results of Table VII.

³⁵ Y. Onodera and T. Toyozawa, J. Phys. Soc. Japan 22, 833 (1967).

VI. CONCLUSIONS

The piezoreflectance technique has been used to obtain values of the shear deformation potentials b and d of the top of the valence band of germanium and a number of materials with zinc-blende structure. Whenever static high-stress data are available, they agree with the small-stress modulation results within the experimental accuracy ($\sim 20\%$). This rules out any significant differences between the small-stress splittings of the exciton and the corresponding band edge.

The ratio of deformation potentials $\eta = d/\sqrt{3}b$, which corresponds to the ratio of valence-band splittings for a given strain along $[100]$ and $[111]$, shows a systematic increase when going from germanium to the III-V and II-VI compounds. This increase must obviously be related to the increasing ionicity of the materials. We have interpreted this increase in η with ionicity as due to the effect of the ionic Coulomb potential on the anisotropic p -like wave functions of the valence band at $\mathbf{k}=0$. A simple displaced-point-ion model was used to calculate the contribution of this Coulomb potential to b and d ; the observed increase in η with ionicity was accounted for on the basis of this model.

Piezoreflectance measurements of the A-B-C exciton spectrum of hexagonal CdS, CdSe, and ZnO yield the ratio of certain combinations of shear (C_3, C_4) to hydrostatic (C_1, C_2) deformation potentials. For CdSe and ZnO, this ratio agrees with that obtained from measurements under large static stress. For CdS, the differential stress measurements indicate that the B exciton moves toward *lower* energies under a small $[11\bar{2}0]$ compression while the large static stress measurements indicate the opposite. Piezoreflectance measurements for modulated stress parallel to $[11\bar{2}0]$ and a reflecting surface perpendicular to the c axis ($\mathbf{K} \parallel c$) yield the stress-exchange splitting of the exciton and the exchange integral J . The values of J obtained for CdS, CdSe, and ZnO are close to those obtained by Onodera and Toyozawa for the alkali halides.

ACKNOWLEDGMENTS

We are grateful to the following individuals and organizations who supplied the samples used for these measurements: A. Fischer of RCA (InP), Juan Montal (natural ZnS), M. I. Nathan of IBM (InP), A. G. Thompson of Bell and Howell (GaAs, GaSb), D. M. Warschauer of NASA (GaAs), and H. H. Woodbury of GE (CdTe). Samples were also obtained from the following commercial suppliers: Clevite (CdSe, CdS), Eagle Picher (ZnS), Litton Industries-Airtron (ZnO), and Minnesota Mining (ZnO). The PZT's were obtained from Clevite. We are also grateful to Dr. F. H. Pollak and Dr. J. E. Rowe for innumerable stimulating discussions.